Photodetachment microscopy of a hydrogen negative ion in an electric field near a metal surface*

Tang Tian-Tian(唐田田), Wang De-Hua(王德华)†, and Wang Shan-Shan(王姗姗)

School of Physics and Optoelectronic Engineering, Ludong University, Yantai 264025*, China*

(Received 19 December 2011; revised manuscript received 27 December 2011)

According to the semi-classical theory, we study the photodetachment microscopy of H^- in the electric field near a metal surface. During the photodetachment, the electron is photo-detached by a laser and the electron is drawn toward a position-sensitive detector. The electron flux distribution is measured as a function of position. Two classical paths lead the ion to any point in the classically allowed region on the detector, and waves traveling along these paths produce an interference pattern. If the metal surface perpendicular to the electric field is added, we find that the interference pattern is related not only to the electron energy and the electric-field strength, but also to the ion–surface distance. In addition, the laser polarization also has a great influence on the electron flux distribution. We present calculations predicting the interference pattern that may be seen in experiment. We hope that our study can provide a new understanding of the electron flux distribution of negative ions in an external field and surface, and can guide future experimental research on negative ion photo-detachment microscopy.

Keywords: photodetachment microscopy, electron flux distribution, semi-classical theory

PACS: 32.80.Gc, 03.65.Sq, 34.35.+a, 07.78.+s **DOI:** 10.1088/1674-1056/21/7/073202

1. Introduction

Photodetachment microscopy is used to measure the electron affinities of atoms and molecules with unprecedented accuracy. Much attention has been paid to photodetachment microscopy since it was first proposed by Demkov *et al.*, who suggested that during the detachment of an electron from a negative ion in the presence of an electric field, the electron would be able to follow several trajectories to the detector, and that this situation would produce an interference pattern.[1,2] The first experimental research on photodetachment microscopy was made by Blondel *et al.*[3] Ejected electrons produced by photodetachment of Br^- in an electric field were recorded with a high resolution detector in the direction perpendicular to the applied electric field. The recorded pattern displayed concentric interference fringes. The measurement with a subsequent detector of photodetachment of O^- in an electric field was also performed by Brondel *et al.*[4] Quantum calculations were shown to be in excellent agreement with the experimental data, allowing the determination of electron affinities from the interference patterns in an unprecedented accuracy.[5−7] In addition, a semi-classical method has been developed by Du[8] to predict outgoing electron current distributions in photodetachment of H^- in an electric field prior to the experiment of Blondel *et al.* An analytical formula for the electron flux distribution has been presented. The oscillations in the spatial distribution of detached electrons have been attributed to the interference of waves propagating along two distinctive paths from the region of the bound state of H^- to the same point. Recently, many investigations on the photodetachment microscopy in the presence of parallel electric and magnetic fields have been reported.[9−11] In these previous studies, they all considered the photodetachment microscopy in the presence of external fields. As to the photodetachment microscopy of H^- near surfaces, no results have been reported. In our previous studies, we have investigated the photodetachment of H^- or wave packet dynamics of photodetachment of H^- in external fields and on metal surface.[12−15] In the present work, using the semi-classical theory,[16−19] we study the photodetachment microscopy of a hydrogen negative ion in the electric field near a metal surface for the first time. Our study suggests that when the metal surface perpendicular to the electric field is added, the inter-

*Project supported by the National Natural Science Foundation of China (Grant Nos. 11074104 and 10604045) and the Higher Educational Science and Technology Program of Shandong Province, China (Grant No. J09LA02).

†Corresponding author. E-mail: jnwdh@sohu.com

© 2012 Chinese Physical Society and IOP Publishing Ltd

ference pattern on the detector is related not only to the electron energy and the electric-field strength, but also to the ion–surface distance. Moreover, the laser polarization also has a great influence on the electron flux distribution. We hope that our study may provide a new understanding of the electron flux distribution of negative ions in external fields near the metal surfaces.

The rest of this paper is organized as follows. In Section 2, we describe the Hamiltonian and the photodetachment process for the system of H^-in an electric field near a metal surface. Then we mainly derive an analytical formula for electron wave function and the distribution of electron flux by using the semiclassical theory. Some calculation results and discussion are given in Section 3. Some conclusions are drawn from the present study in Section 4. Atomic units are used throughout this paper unless otherwise indicated.

2. Theory and method

Assuming that the hydrogen negative ion is located at the origin. A laser is used for the photodetachment and a metal surface is kept in the $z = -d$ plane. An external electric field F perpendicular to the metal surface is applied. A position-sensitive detector is placed in the $z = -z_0$ plane. The Hamiltonian H for the detached electron in the electric field near a metal surface has the following form (in cylindrical coordinates):[20]

$$H = \frac{1}{2}P_\rho^2 + \frac{1}{2}P_z^2 - \frac{1}{4(d+z)} + \frac{1}{4d} + Fz, \quad (1)$$

where d is the distance between the hydrogen negative ion and the metal surface, and F is the electric-field strength.

The photodetachment process of H^- in this system can be described as follows. When a laser is applied to H^-, the ion may absorb a photon, then the detached electron becomes an outgoing p-wave. This wave propagates away from the ion. The wave propagates sufficiently far from the ion according to the semi-classical mechanics, and it is correlated with classical trajectories. Due to the effects of electric field and the metal surface, the waves initially propagating away from the ion will return back, and then propagate to large distances down field to interfere with the initial waves, giving rise to a two-term interference pattern in the electron flux distribution on the detector.

The hydrogen negative ion is considered as a one-electron system. The electron is bounded by a short-range potential. The binding energy of the electron E_b is 0.754 eV, and the laser photon energy $E_\mathrm{ph} = E + E_\mathrm{b}$, where E is the electron energy.[16] Let the initial bound state of H^- be $\phi_\mathrm{i}(r) = Br^{-1}\exp(-k_\mathrm{b}r)$, with $B = 0.31552$ and $k_\mathrm{b} = 0.2344883$ as previously used in Refs. [17]–[19]. The electron outgoing wave ψ_f produced in the photodetachment in the presence of electric field near a metal surface satisfies the following inhomogeneous Schrödinger equation:

$$(E - H)\psi_\mathrm{f} = D\phi_\mathrm{i}, \quad (2)$$

where D is the dipole operator. For an arbitrary laser polarization, we assume that the laser polarization is along the $(\theta_\mathrm{L}, \varphi_\mathrm{L})$ direction. The dipole operator D can be written in the following form:

$$\begin{aligned} D &= \boldsymbol{r}\cdot\boldsymbol{\varepsilon} \\ &= r(\sin\theta\cos\varphi, \sin\theta\sin\varphi, \cos\theta) \\ &\quad \cdot (\sin\theta_\mathrm{L}\cos\varphi_\mathrm{L}, \sin\theta_\mathrm{L}\sin\varphi_\mathrm{L}, \cos\theta_\mathrm{L}) \\ &= rf(\theta, \varphi; \theta_\mathrm{L}, \varphi_\mathrm{L}), \end{aligned} \quad (3)$$

where $f(\theta, \varphi; \theta_\mathrm{L}, \phi_\mathrm{L})$ represents the dependence of the detached electron wave function on the outgoing direction (θ, ϕ),[21] i.e.,

$$\begin{aligned} f(\theta, \varphi; \theta_\mathrm{L}, \phi_\mathrm{L}) &= \cos\theta\cos\theta_\mathrm{L} \\ &\quad + \sin\theta\sin\theta_\mathrm{L}\cos(\varphi - \varphi_\mathrm{L}). \end{aligned} \quad (4)$$

Assuming the detector perpendicular to the z axis and intersect with the axis at $z < 0$, the detached-electron flux distribution on this detector can be calculated according to[8]

$$\begin{aligned} \frac{\mathrm{d}^2\sigma(\rho, z, \varphi)}{\rho\mathrm{d}\rho\mathrm{d}\varphi} &= -\frac{2\pi(E_\mathrm{b} + E)}{c}\boldsymbol{j}\cdot\boldsymbol{k}, \\ \boldsymbol{j} &= \frac{\mathrm{i}}{2}(\psi_\mathrm{f}\boldsymbol{\nabla}\psi_\mathrm{f}^* - \psi_\mathrm{f}^*\boldsymbol{\nabla}\psi_\mathrm{f}), \end{aligned} \quad (5)$$

where ψ_f is the detached electron wave function, and $\boldsymbol{k}$ is a unit vector perpendicular to the detector.

2.1. Detached electron wave function

The outgoing electron wave function in the photodetachment of H^- in the absence of electric field $\psi_\mathrm{out}(\boldsymbol{r})$ satisfies

$$\Big[E + \frac{1}{2}\boldsymbol{\nabla}^2 - V_\mathrm{p}(\boldsymbol{r})\Big]\psi_\mathrm{out}(\boldsymbol{r}) = D\phi_\mathrm{i}, \quad (6)$$

where $V_\mathrm{p}(\boldsymbol{r})$ is the polarized central field of the H atom. Since φ_i is an S state for H^-, outside the source region, we have[8]

$$\psi_\mathrm{out}(\boldsymbol{r}) = \Big[\sum_{m=-1}^{1} C_m(k)Y_{1m}(\theta, \varphi)\Big]h_1^{(1)}(kr), \quad (7)$$

with

$$C_m(k) \equiv -2\mathrm{i}k \int j_1(kr) Y^*_{1m}(\theta,\varphi) D(r) \phi_\mathrm{i}(r) \mathrm{d}V, \quad (8)$$

where $j_1(kr)$ and $h_1^{(1)}(kr)$ are the regular and outgoing spherical Bessel functions, respectively. By using the integral $\int_0^\infty j_1(kr)\,\mathrm{e}^{-k_\mathrm{b}r} r^2 \mathrm{d}r = 2k(k_\mathrm{b}^2+k^2)^{-2}$, then Eq. (7) becomes

$$\psi_\mathrm{out}(\boldsymbol{r}) = -\frac{4\mathrm{i}k^2 B}{(k_\mathrm{b}^2+k^2)^2} f(\theta,\varphi;\theta_\mathrm{L},\varphi_\mathrm{L}) h_1^{(1)}(kr). \quad (9)$$

At large r, the following asymptotic form is used:

$$h_1^{(1)}(kr) \sim \frac{1}{kr}\exp[\mathrm{i}(kr-\pi)], \quad r\to\infty. \quad (10)$$

Finally, we obtain the expression of $\psi_\mathrm{out}(r)$ in the following form:

$$\psi_\mathrm{out}(r,\theta,\varphi) = -\frac{4\mathrm{i}k^2 B}{(k_\mathrm{b}^2+k^2)^2} f(\theta,\varphi;\theta_\mathrm{L},\varphi_\mathrm{L}) \frac{\exp(\mathrm{i}kr)}{kr}. \quad (11)$$

As the electron wave propagates out to large r, the influences of electric field and metal surface become more and more important. Therefore, we can neglect the influence of the short-range potential of the detached electron on the hydrogen atom and use the semi-classical method to compute the outgoing wave function, which is related to the classical trajectories of the photo-detached electron. In cylindrical coordinates, the classical motion of the detached electron in the electric field near a metal surface can be separated into the motion along the z axis and the motion along the ρ axis. Then the classical motion equations can be formally written as

$$\rho(t) = r(\sin\theta) + k(\sin\theta)t,$$
$$z(t) = \int_0^t \sqrt{2\Big(E\cos^2\theta + \frac{1}{4(d+z)} - \frac{1}{4d} - Fz\Big)}\,\mathrm{d}t. \quad (12)$$

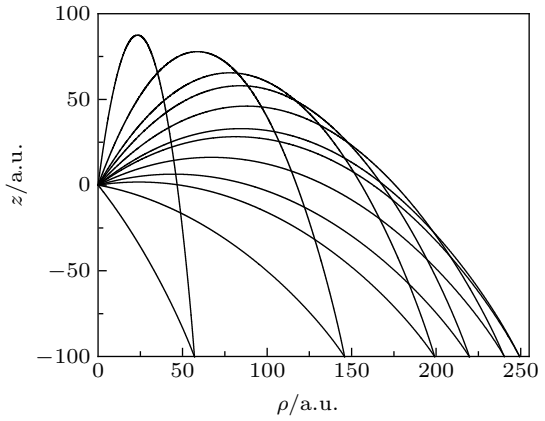


Fig. 1. Some outgoing electron trajectories in the photo-detached electron flux of H^- in the electric field near a metal surface. The observation plane is placed at $z = -100$ a.u. The metal surface is placed at $z = -120$ a.u.

Figure 1 shows some of the electron trajectories described by Eq. (12) with varying θ. Due to the effects of the metal surface and the electric field, there are two distinctive trajectories along which the electron waves produced in the photodetachment in the bound state region of H^- propagate to arrive at the same point on the detector plane. Thus, the wave function at a given point (ρ, z, ϕ) can be written as the sum of the contributions from the two trajectories[8,19]

$$\psi_\mathrm{f}(\rho,z,\varphi) = \sum_{j=1}^{2} \psi_\mathrm{out}(r,\theta_j,\varphi) A_j(\rho,z,\varphi) \times \exp\Big[\mathrm{i}\Big(S_j(\rho,z,\varphi) - \frac{\mu_j\pi}{2}\Big)\Big], \quad (13)$$

where A_j is the corresponding amplitude and can be written as[22]

$$A_j = \left|\frac{\det J_j^{(2)}(\rho,z,0)}{\det J_j^{(2)}(\rho,z,t)}\right|^{1/2} \left|\frac{\rho(0)}{\rho(t)}\right|^{1/2},$$

with $J^{(2)}(\rho,z,t)$ being a two-dimensional Jacobian[23]

$$J^{(2)}(\rho,z,t) = \begin{pmatrix} \dfrac{\partial\rho}{\partial t} & \dfrac{\partial z}{\partial t} \\ \dfrac{\partial\rho}{\partial\theta} & \dfrac{\partial z}{\partial\theta} \end{pmatrix}.$$

Then, we have

$$A_j = \sqrt{\frac{kr^2\sin\theta_j}{\rho(t)\Big(\dfrac{\partial z}{\partial t}\dfrac{\partial\rho}{\partial\theta} - \dfrac{\partial\rho}{\partial t}\dfrac{\partial z}{\partial\theta}\Big)}}. \quad (14)$$

In Eq. (13), $S_j = \int p_\rho \mathrm{d}\rho + \int p_z \mathrm{d}z$ is the classical action, and μ_j is the Maslov index of the j-th trajectory.

2.2. Detached electron flux distribution

Now consider a detector plane perpendicular to the electric field that intersects with the z axis at $z<0$. The resulting wave function, given quantitatively by Eq. (13), is therefore a sum of two terms. Inserting Eq. (13) into Eq. (5), the differential cross section or the electron flux distribution exhibit a typical two-term interference pattern. The electron flux distribution defined on this detector plane may be readily evaluated from Eqs. (13) and (5) as

$$\frac{\mathrm{d}^2\sigma(\rho,z,\varphi)}{\rho\mathrm{d}\rho\mathrm{d}\varphi} = -\frac{2\pi(E_\mathrm{b}+E)}{c}\Big[|\psi_\mathrm{f1}|^2 v_{1z} + |\psi_\mathrm{f2}|^2 v_{2z} + (v_{1z}+v_{2z})\mathrm{Re}(\psi_\mathrm{f1}\psi_\mathrm{f2}^*)\Big], \quad (15)$$

where

$$\psi_{\mathrm{f}j} = -\frac{4\mathrm{i}k^2 B}{(k_{\mathrm{b}}^2+k^2)} f(\theta_j,\varphi;\theta_{\mathrm{L}},\varphi_{\mathrm{L}})\frac{\mathrm{e}^{\mathrm{i}kr}}{k}\mathrm{e}^{\mathrm{i}(S_j-\mu_j\pi/2)} \times \sqrt{\frac{k\sin\theta_j}{\rho(t)(\frac{\partial z}{\partial t}\frac{\partial\rho}{\partial\theta}-\frac{\partial\rho}{\partial t}\frac{\partial z}{\partial\theta})}},\ j=1,2, \qquad (16)$$

and v_{1z} and v_{2z} are the z components of the electron velocities of trajectories 1 and 2 at (ρ, z, ϕ), respectively.

3. Results and discussion

Using Eq. (15), we calculate the electron flux distribution of H^- in electric field near a metal surface. Firstly, we consider the case of the laser polarization parallel to the z axis, which corresponds to the case of $\theta_{\mathrm{L}} = 0$. In Fig. 2, we study the influence of the ion–surface distance d on the electron flux distribution. The detached electron energy $E = 0.26$ eV, the electric-field strength $F = 500$ kv/cm and the detector plane is fixed at $z = -100$ a.u.

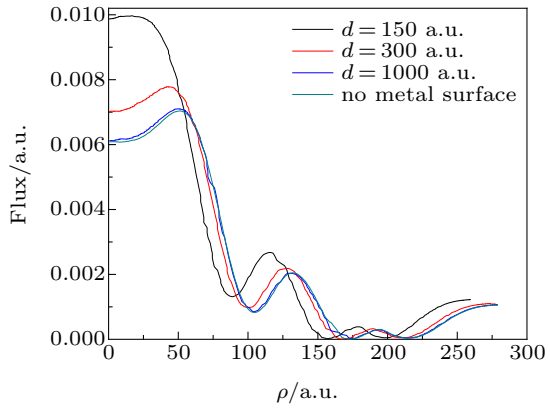


Fig. 2. (colour online) Electron fluxes of H^- in the electric field near a metal surface with different values of ion–surface distance d.

The results suggest that with the increase of the ion–surface distance d, the oscillating amplitude in the electron flux distribution decreases and the oscillating peaks shift toward the right on the whole simultaneously. The impact radius of the electron reaching the detector plane increases. For example, for ion–surface distance $d = 150$ a.u., the maximum oscillating amplitude in electron flux distribution is 0.01 a.u., and the corresponding position is at $\rho = 14.9$ a.u. When the ion–surface distance d increases to 300 a.u., the maximum oscillating amplitude in electron flux decreases to 0.008 a.u., and the corresponding position shifts to $\rho = 43.8$ a.u. If the ion–surface distance continues to increase to 1000 a.u., the electron flux of H^- is close to that in the case where only electric field exists and the influence of the metal surface can be neglected.[8] It can be interpreted as follows: when the ion–surface distance d increases, the electrostatic potential of the metal surface acting on the detached electron reduces. The electron needs to move farther to reach the detector plane. Then, the strengths of outgoing waves in the detector plane emitting from the H^- are weak. As a result, the interference effect is reduced and the impact radius increases. When the ion–surface distance increases to 1000 a.u., the electrostatic attraction potential of the metal surface is very small so that the electron flux under this condition is coincident with the case where only electric field exists.

In Fig. 3, we display the electron flux of H^- with fixed ion–surface distance d and electric-field strength, but with different values of detached electron energy E. This figure suggests that as the electron energy changes, the amplitude in the electron flux near the z axis ($\rho \approx 0$) varies and the impact radius of the electron arriving at the detector plane increases. In addition, the oscillation patterns at large ρ remain similar in shape, but shift slightly for different electron energies.

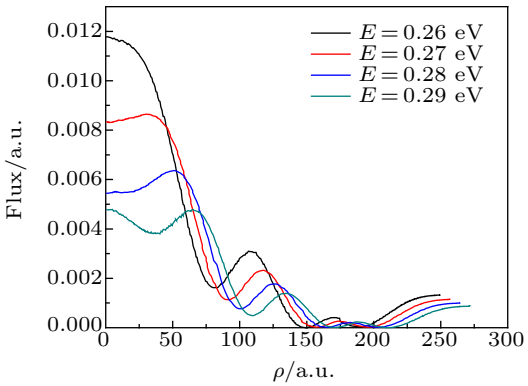


Fig. 3. (colour online) Electron fluxes of H^- in the electric field near a metal surface at different electron energies. The ion–surface distance d is 120 a.u. The observation plane is placed at $z = -100$ a.u. The electric field strength $F = 500$ kv/cm.

Figure 4 shows the electron fluxes of H^- with a given ion–surface distance d and detached electron energy, but with different electric field strengths. Moreover, the electric-field strength F is 300 kv/cm, the number of the peaks in the flux is 5 and the maximum impact radius of the electron arriving at the detector plane is 350 a.u. With the increase of the electric field strength, the number of the peaks in the electron flux distribution decreases and the maximum impact radius of the electron arriving at the detector plane also decreases correspondingly. When the electric field strength increases to 700 kv/cm, the number

of the peaks in oscillation decreases to 3 and the maximum impact radius of the electron arriving at the detector plane decreases to 200 a.u.

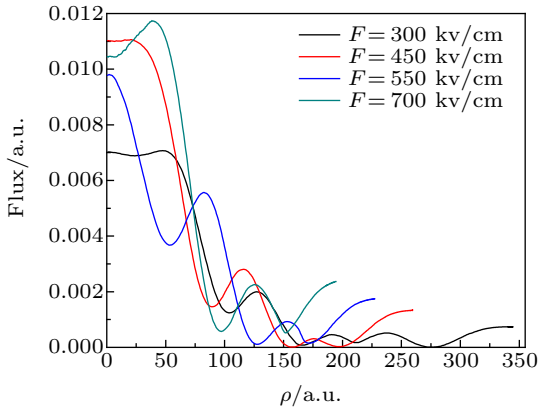


Fig. 4. (colour online) Electron fluxes of H^- in the electric field near a metal surface with different electric-field strengths. The ion–surface distance d is 120 a.u. and the electron energy $E = 0.25$ eV. The observation plane is placed at $z = -100$ a.u. The electric-field strengths are 300, 450, 550, and 700 kv/cm, respectively.

In order to show the electron flux distribution on the detector plane clearly, we plot the three-dimensional contour interference fringes (see Fig. 5). Such interference patterns are similar to the ones observed in the "photodetachment microscopy" experiments.[3,4,7] It is found that the three-dimensional contour interference fringes on the detector consist of bright and dark rings. The bright ring which corresponds to the peak appears at the detector plane because of constructive interference of the two coherent detached-electron waves, and the dark ring which corresponds to valley appears at the detector plane because of destructive interference of the two coherent detached-electron waves. With the increase of the electric field strength, the maximum impact radius of the ring decreases. For instance, when the electric-field strength F increases to 700 kv/cm, the maximum impact radius becomes small, and thus the concentric interference fringes become much smaller. The results are in excellent agreement with the results shown in Fig. 4.

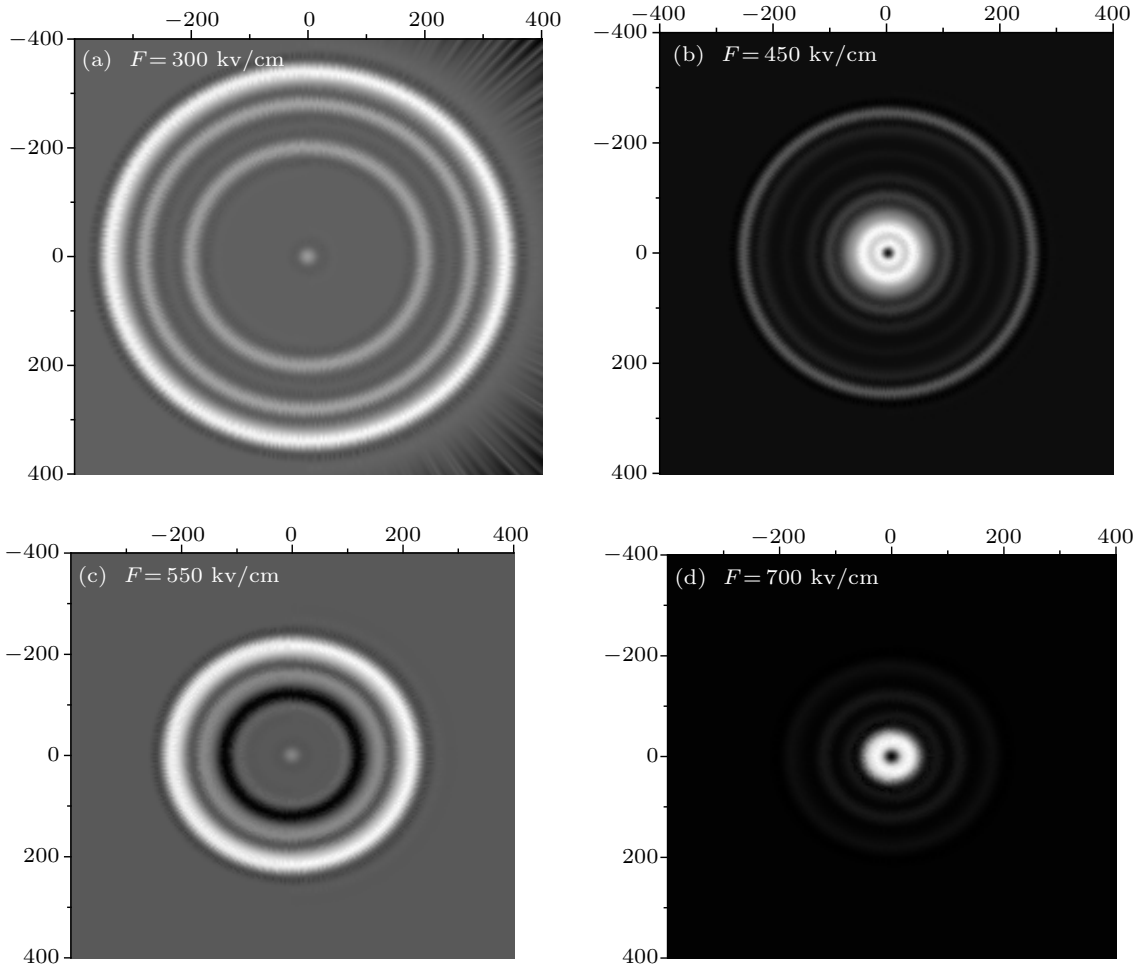


Fig. 5. Three-dimensional contour interference fringes on the observation plane for (a) $F = 300$, (b) 450, (c) 550, and (d) 700 kv/cm, corresponding to Fig. 4.

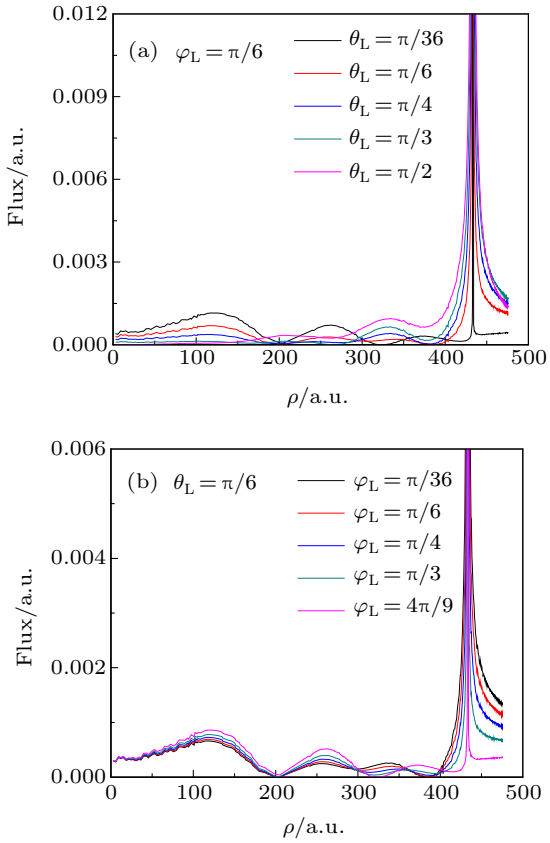


Fig. 6. (colour online) The electron fluxes of H^- in the electric field near a metal surface when the laser polarization is in the (θ_L, ϕ_L) direction. (a) $\phi_L = \pi/6$. (b) Polarization angle $\theta_L = \pi/6$.

Finally, we study the laser polarization effect on the electron flux distribution of H^- in electric field near a metal surface. The result is demonstrated in Fig. 6. Let the ion–surface distance $d = 500$ a.u., electron energy $E = 0.26$ eV, and electric-field strength $F = 500$ kv/cm. The detector plane is placed at $z = -490$ a.u. Due to the cylindrical symmetry of the system, we take ϕ to be zero for convenience. Firstly, we keep the azimuth angle unchanged ($\phi_L = \pi/6$), and vary the value of θ_L. The results are given in Fig. 6(a). From this figure we find that there is a boundary angle of $\pi/4$. When the value of θ_L is less than $\pi/4$, taking $\theta_L = \pi/6$ for example, the amplitude of the oscillation in the electron flux first decreases and then increases until a large oscillation appears. However, when the value of θ_L is greater than $\pi/4$, taking $\theta_L = \pi/3$ for example, the amplitude of the oscillation in the electron flux is almost invisible and then continues to increase until a large oscillation appears. In the following case, we fix the polarization angle θ_L to be $\pi/6$ and change the azimuth angle ϕ_L. The results are given in Fig. 6(b). This figure indicates that the amplitude in the electron flux changes with the increase of the azimuth angle ϕ_L, but the change is very small. In addition, the oscillation patterns are nearly similar in shape. The result suggests that the azimuth angle ϕ_L has a little effect on the electron flux distribution. Comparing Fig. 6(a) with Fig. 6(b), we find that the influence of the polarization angle θ_L on the electron flux distribution is more obvious than the influence of the azimuth angle ϕ_L. In other words, the effect of the polarization angle θ_L on the electron flux distribution is more important.

4. Conclusion

We study the photodetachment electron flux of hydrogen negative ions in the electric field near a metal surface by using the semi-classical method. The results show that the detached-electron waves traveling along two distinct paths lead to the interference in the electron flux distribution. The calculation results suggest that if the metal surface perpendicular to the electric field is added, the interference pattern in the electron flux distribution is related not only to the electron energy and the electric field strength, but also to the ion–surface distance. Moreover, the laser polarization effect on the electron flux distribution is also discussed. The results show that the influence of the polarization angle θ_L on the electron flux is more obvious than the influence of the azimuth angle ϕ_L. Since no experiment on the photodetachment microscope of H^- in this system has been carried out, we hope this theoretical prediction will guide future experiments on the photodetachment microscopy.

References

[1] Demkov Y N, Kondratovich V D and Ostrovskii V N 1981 *JETP Lett.* **34** 403
[2] Bracher C, Becker W, Gurvitz S A, Kleber M and Marinov M S 1998 *Am. J. Phys.* **66** 38
[3] Blondel C, Delsart C and Dulieu F 1996 *Phys. Rev. Lett.* **77** 3755
[4] Blondel C, Delsart C, Dulieu F and Valli C 1999 *Eur. Phys. J.* D **51** 207
[5] Kramer T, Bracher C and Kleber M 2002 *J. Phys.* A **35** 8361
[6] Valli C, Blondel C and Delsart C 1999 *Phys. Rev.* A **59** 3809
[7] Blondel C, Chaibi W, Delsart C, Drag C, Goldfarb F and Kröger S 2005 *Eur. Phys. J.* D **33** 335
[8] Du M L 1989 *Phys. Rev.* A **40** 4984
[9] Kramer T, Bracher C and Kleber M 2001 *Europhys. Lett.* **56** 471
[10] Bracher C, Kramer T and Delos J B 2006 *Phys. Rev.* A **73** 062114
[11] Bracher C and Delos J B 2006 *Phys. Rev. Lett.* **96** 100404
[12] Huang K Y and Wang D H 2010 *Chin. Phys.* B **19** 063402

[13] Wang S S, Wang D H, Huang K Y and Tang T T 2011 *Acta Phys. Sin.* **60** 103401 (in Chinese)
[14] Tang T T, Wang D H, Huang K Y and Wang S S 2011 *Chin. Phys.* B **20** 063205
[15] Wang S S, Wang D H, Huang K Y and Tang T T 2011 *Acta Phys. Sin.* **60** 053402 (in Chinese)
[16] Du M L and Delos J B 1987 *Phys. Rev. Lett.* **58** 1731
[17] Du M L and Delos J B 1988 *Phys. Rev.* A **38** 1896
[18] Du M L and Delos J B 1988 *Phys. Rev.* A **38** 1913
[19] Du M L and Delos J B 1988 *Phys. Rev.* A **38** 5609
[20] Yang B C and Du M L J 2010 *J. Phys.* B **43** 035002
[21] Du M L 2006 *Eur. Phys. J.* D **38** 533
[22] Yang G C and Du M L 2000 *Commun. Theor. Phys.* **33** 1
[23] Peters A D, Jaffé C and Delos J B 1997 *Phys. Rev.* A **56** 331